Detection of Orbital Debris Using Self-Interference Cancellation Residual Signal

S. Jayasimha and P. Jyothendar
Signion Systems
IDA Bollaram, Medak, India

***Abstract*—We show that large-antenna earth-stations, communicating with geo-stationary satellite-relays and re-using spectrum via self-interference cancellation, can detect line-of-sight orbital debris. Higher frequency signals can spot and range debris as small as 5cm in diameter. We also provide new insights into the influence of weather and orbital debris on self-interference canceller performance.**

Keywords- Bi-static radar; Doppler; Forward-scatter; Ka-band; LEO; Orbital debris; Self-interference cancellation

I. INTRODUCTION

In debris-rich low-earth orbits (LEO), the production rate of new debris due to collisions exceeds objects lost to orbital decay [1]. Strategically located radar and optical sensors, the U.S. Space Surveillance Network (SSN), reliably tracks and catalogues orbital debris (OD) greater than 10cm in size. We examine OD signatures on existing geosynchronous (GEO) commercial satellite and teleport communications signals. Detection and ranging of LEO OD transits could augment and perhaps even improve reliability of, the SSN catalogue.

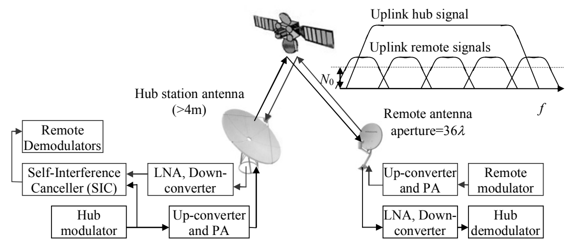

Figure 1. Duplex communications with self-interference canceller

At higher frequencies (e.g., Ka band, 30GHz and 20GHz for up- and down-link respectively), transponders/ teleports using *self-interference cancellers* [2, 3] (SICs), could identify and range objects transiting near the teleport to satellite line-of-sight (LOS). Fig. 1 shows an overlapped transmission band of large aperture hub and a very small aperture terminal (VSAT). At the hub receiver, the VSAT signal's power spectral density (PSD) is usually smaller than the hub signal by approximately the hub-to-VSAT antenna gain ratio. The VSAT signal is demodulated after the hub's received signal is processed by the SIC.

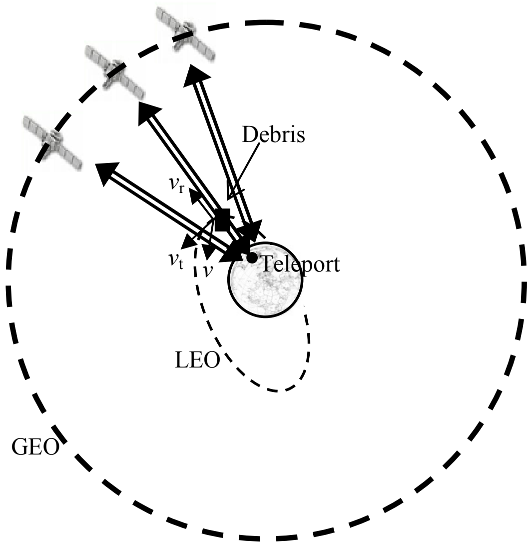

Figure 2. Antennas at each teleport pointing to different satellites

If each of N teleports (in 2010, their world-wide number was 1740 [4]) communicate with K GEO satellites[1], then $N{\cdot}K$ sky look angles would simultaneously be examined as in Fig. 2. Antenna point angles (in azimuth and elevation), together with teleport location (latitude/ longitude) and debris range obtain the orbital plane, while other fixes on the same object (assuming no collisions between observations,

[1] Teleports can also communicate via non-GEO satellite constellation relays; however, hand-off between satellites in the constellation must be "seamless", i.e., continuous in group-delay and Doppler, to use SIC

correlating sighting-time, direction and range), as shown in Fig. 3, allows calculation of orbital eccentricity and semi-major axis [5]. Teleports thus co-operating with the SSN could augment and authenticate LEO space debris database more frequently.

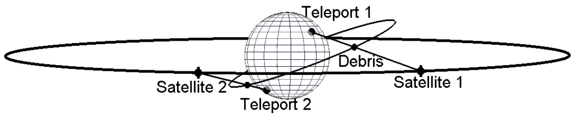

Figure 3. One range measurement defines orbital plane; observations from other teleports may allow semi-major axis and eccentricity determination

II. Sensor Principle

In forward scattering [6], incident and scattered signals interfere in a wave-front "hole" shadow region. By Babinet's principle, this body-material independent forward-scattering radar cross-section (FSRCS, σ) exceeds back-scatter (e.g., pp. 65-66 of [7]) by orders of magnitude; an object of silhouette-area A intersecting a λ-wavelength beam (i.e., bi-static angle nearly 180°) has FSRCS:

$$\sigma = 4\pi(A/\lambda)^2 \qquad (1)$$

A 10cm diameter (d) object at 30GHz (uplink) has FSRCS of 7.75m^2 or 9dBsm and at 20GHz (downlink) an FSRCS of 3.45m^2 or 5.4dBsm (in comparison, a d=5cm object has FSRCS of 0.48m^2 or -3.1dBsm on the uplink and 0.22m^2 or -6.7dBsm on the downlink). Because the cone-angle, θ, of forward-scattering is small, FSRCS greatly exceeds back-scatter RCS [8]:

$$\theta = (\lambda/d)\cdot(180/\pi) \qquad (2)$$

At 30GHz, the forward-scatter beam-width is 5.7° and 10.4° for 10cm and 5cm objects respectively.

High-gain, fractional-degree (<0.3°) beam-width Ka-band teleport antennas partly compensate atmospheric rain fades [9]. High-throughput satellites (HTS) Ka-band spot beams have 0.5-1° 3dB beam-widths. At LEO ranges, the *loop-back* uplink beam is larger than the downlink beam (Fig. 4, where debris paths crossing the intersection of the uplink transmit and receive beams) mainly due to the earth-station's transmit/ receive beam-span being much smaller than the satellite's transmit/ receive beam-span. However, in Ka-band the uplink beam is smaller than downlink beam because of the factor of 1.5 in the uplink/ downlink frequencies. At LEO ranges, the uplink and downlink beams are nearly concentric as they are determined mainly by the much closer earth-station antenna.

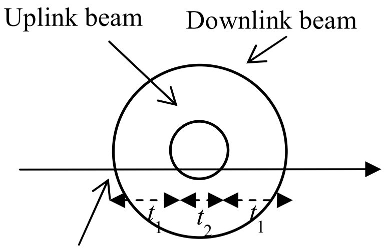

At debris range, r_d and tangential velocity, v_t

Figure 4. Debris traversing teleport and satellite beams

When debris transits near-LOS, a direct path and at least one attenuated, Doppler-shifted forward-scattered path exists. These effect the SIC at times shown in Figures 5 and 6a; assuming uniform debris velocity and $t_1 > 2T_{ds}$, a) due to downlink scattering at T_1, b) due to both the up and down-link scattering beginning $T_2 = T_1 + t_1 + 2T_{ds}$,, c) only downlink scattering from $T_3 = T_2 + t_2$ to $T_4 = T_3 + t_1 - 2T_{ds}$. Similarly, Fig. 6b shows the $t_1 < 2T_{ds}$ case. Solving the three linear equations, hinging on the two beams being nearly concentric, yields t_1, t_2 and, particularly relevant, $2T_{ds}$.

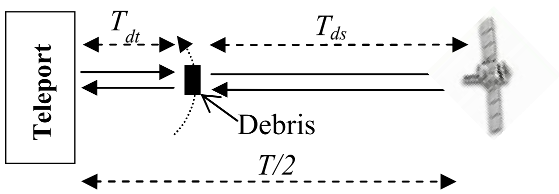

Figure 5. Debris-scattered signals at SIC's output

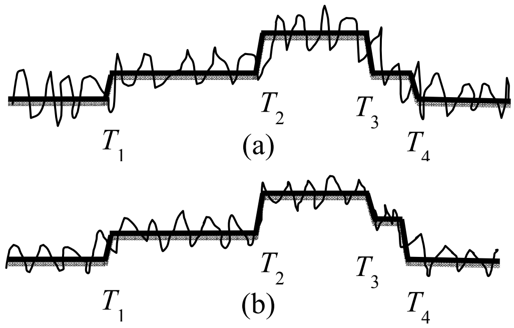

Figure 6. Post-SIC envelope detector

For debris radial velocity v_r, the Doppler is $f_c v_r / c$, where f_c is the up-/ down-link carrier frequency and c the propagation-speed; e.g., Doppler of 100kHz (assuming f_c=30GHz and v_r=1km/s) greatly exceeds the SIC's phase-locked loop (PLL) bandwidth; thus, SIC only cancels the direct path signal and its output contains one or two debris-scattered signals, causing brief interference to the inbound signal (from small-aperture remote earth-stations) in SIC-based frequency re-use systems.

With effective average radiated power, P, typically 55-58dBW for satellite antenna and 86-89dBW for 6.3-8.1m teleport antenna, integration time, τ, transmit and receive antenna gains, G_t and G_r, typically 62-65dB receive/ transmit at the teleport, typically 31-34dB receive/ transmit at the satellite, wavelength, λ, FSRCS, σ, teleport-to-debris distance, U, debris-to-satellite distance, R, loss, L, Boltzmann's constant, k, noise temperature, θ and F, the receiver noise figure, the bi-static radar equation yields signal-to-noise ratio (SNR) of the forward-scattered signals:

$$SNR = \frac{P G_t G_r \tau \lambda^2 \sigma}{(4\pi)^3 U^2 R^2 L k T_N F} \qquad (3)$$

SNR, when 10cm-size debris intersects the uplink beam, could be as low as -1dB (-4.5dB for downlink) in adverse weather for τ=0.2s. Ka-band signals are primarily affected in the troposphere. Rain (12dB) and cloud (2dB) attenuation and atmospheric scintillation (0.5dB) are accounted for in the 15dB loss. Although cloud up-/ down-drafts (both on up- and down-links) cause additional Doppler-shifted clutter, debris and air (<20m/s [10, Table 1]) velocity's radial components are widely-separated. However, the debris' signature could be corrupted by direct-path interference due to inadequate cancellation caused by weather-induced clutter being within the SIC's PLL bandwidth.

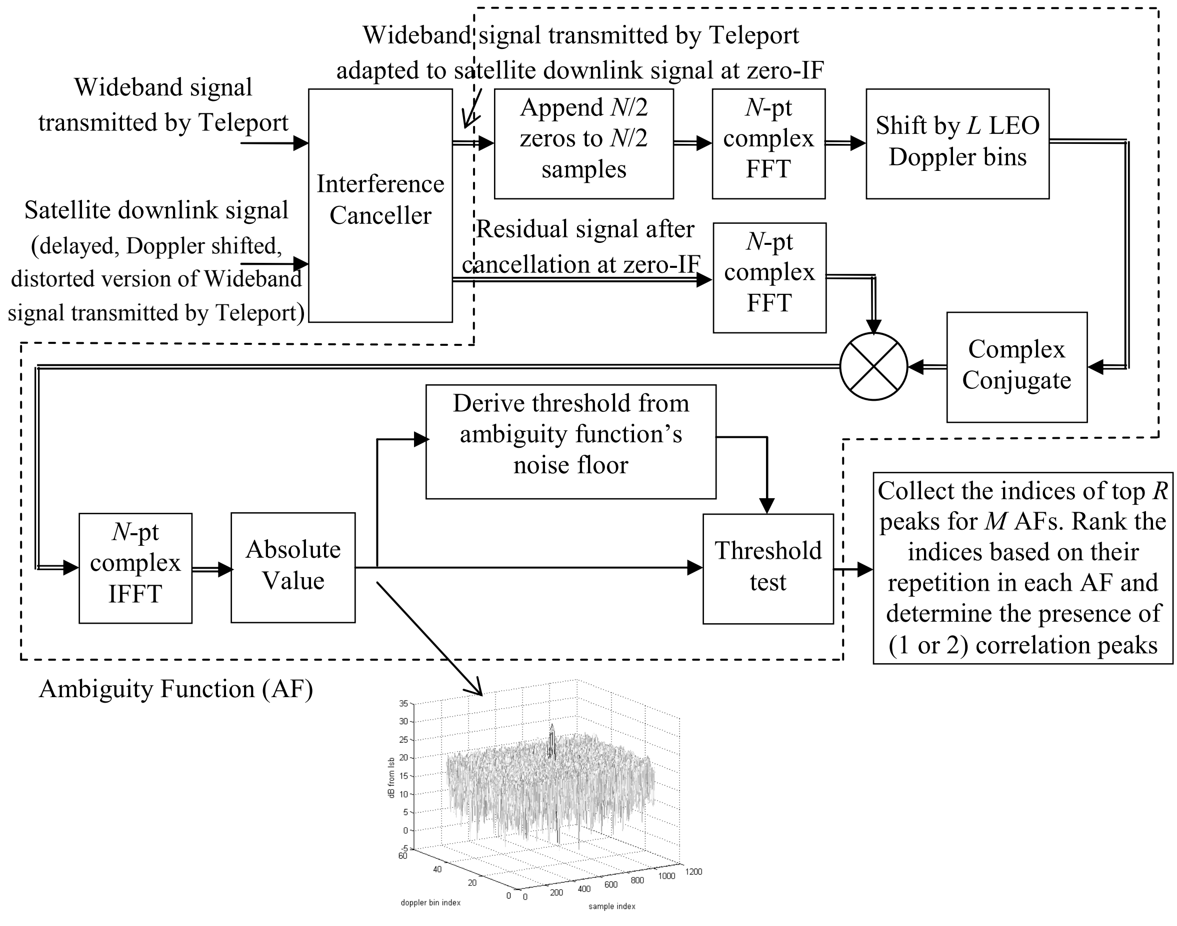

Figure 7. Doppler correlation to detect debris

III. Signature Detector

Fig. 6's envelope detector is sub-optimum, particularly for negative SNR's. Instead, [11]'s cross-ambiguity function (CAF), where τ times signal bandwidth B greatly exceeds uncertainty in range and Doppler product, is computed (Fig. 7) from the SIC's residual signal. The short-duration (<0.5s) uplink signal is double-Doppler-shifted, while the long-duration (5-10s) downlink signal has smaller single Doppler-shift. Range (resolution limited by CAF computation frequency) is obtained from transition times of the debris' tri-symbol signature. An N-sample periodogram at sampling rate, f_s, has a Doppler resolution of f_s/N. We can compute M overlapped CAFs, with overlap factor [12] P, and transit time resolution $MN/(Pf_s)$. With 1km/s debris radial velocity, down- and up-link Doppler are 66kHz and 166kHz respectively. Selecting f_s=70MHz, N=1024, M=3 and P=8, range resolution is ±420m with 14.6μs scattering delay-spread and 68.4kHz Doppler resolution.

For a saturated transponder, residual self-interference, with or without OD, is greatly reduced by applying an estimate of the satellite distortion to the reference outbound signal [3, 13]. In addition, the use of this distorted outbound reference signal also improves the detectability of OD (as indicated in Fig.7). However, when OD is present, SNR in (3) will be degraded due to un-cancelled intermodulation.

IV. Multiple Scattering

The foregoing discussion assumes that OD is sufficiently dispersed that only single forward scattering is present. In some cases, OD can have many closely-spaced fragments, all moving at the same velocity. *Independent scattering* occurs if the space debris fragments are much smaller than, as well as spaced apart by distances much greater than, the illuminating wavelength, in which case the overall intensity is just the superposition of the individual fragments' intensities. More likely, when fragments are of similar or larger size compared to the illuminating wavelength, more complex multiple scattering effects must be considered [14] in arriving at the overall intensity. However, Fig. 7's time and frequency cross-correlation will detect OD in all cases with sufficient overall intensity.

V. Conclusion

We have analyzed the effect of LOS OD on frequency-reuse satellite-relay communications in the context of bi-static forward-scatter radar. We have also shown, using a single-scatterer model, that the SIC's means to acquire negative SNR (e.g., spread spectrum signals) can be used to acquire OD signatures. Finally, we have provided additional insights on SIC performance in the presence of OD of weather-induced Doppler and transponder saturation.

References

[1] D.J. Kessler and B.G. Cour-Palais, "Collision Frequency of Artificial Satellites: The Creation of a Debris Belt," *Journal of Geophysical Research* 83: pp. 2637-2646, 1978.

[2] U.S. Patent 6,859,641 B2: G.D. Collins, D.L. Anair and M.J. Ready, "Adaptive Canceller for Frequency Reuse Systems," February 22, 2005.

[3] U.S. Patents 7,522,877, 7,729,657 and 8,238,817: A. Avellan, S. Godoy, S. Jayasimha and P. Jyothendar "Noise Reduction System and Method Thereof", April 21, 2009, June 1, 2010 and August 7, 2012

[4] "Sizing the Teleport Market 2010," World Teleport Association, December 2010.

[5] S.J. Goldstein, Jr. and R.M. Goldstein, "Some Properties of Millimetric Space Debris," *The Astronomical Journal*, Vol. 107, No. 1, 1994, pp. 367-371.

[6] M.I. Skolnik, *Introduction to Radar Systems*, Second Edition, McGraw-Hill, ISBN 0-07-057909-1, 1980, pp. 557-559.

[7] *Handbook for Limiting Orbital Debris*, NASA-Handbook 8719.14, July, 2008.

[8] Glaser, J.I., "Bi-static RCS of Complex Objects near Forward Scatter," *IEEE Trans. on Aerospace and Electronic Systems*, Vol. AES-21, No. 1, Jan. 1985.

[9] Model 8.1m Satcom Ka-band Cassegrain Antenna data sheet, General Dynamics Satcom Technologies, www.gdsatcom.com, 2012.

[10] P. Kollias, E.E. Clothiaux, B.A. Albrecht, M.A. Miller, K.P. Moran and K.L. Johnson, "The Atmospheric Radiation Measurement Program Cloud Profiling Radars: An Evaluation of Signal Processing and Sampling Strategies," *Journal of Atmospheric and Oceanic Technology*, Vol. 22, July, 2005, pp.930-948.

[11] S. Stein, "Algorithms for Ambiguity Function Processing," *IEEE Trans. on Acoustics, Speech and Signal Processing*, Vol. ASSP-29, NO. 3, June 1981.

[12] J.G. Proakis, C.M. Radar, F. Ling and C.L. Nikias, *Advanced Digital Signal Processing*, Macmillan Publishing Company, 1992, pp. 488-491.

[13] S. Jayasimha and P. Jyothendar, "Cancelling Echoes distorted by Satellite Transponders," Proc. of *National Conference on Communications (NCC-2006)* pp. 112-116, Omega Scientific Publishers, New Delhi, ISBN 81-85399-80-8.

[14] J. Groenenboom and R. Snieder, "Attenuation, dispersion, and anisotropy by multiple scattering of transmitted waves through distributions of scatterers", *Journal of the Acoustical Society of Am*erica, Vol. 98, Issue 6, Dec. 1995, pp. 3482-3492.